Sensors & Actuators: B. Chemical 326 (2021) 128817

Contents lists available at ScienceDirect

Sensors and Actuators: B. Chemical

journal homepage: www.elsevier.com/locate/snb

BTEX gas sensor based on hematite microrhombuses

Luís F. da Silva [a,*], Ariadne C. Catto [a,b], Sandrine Bernardini [c], Tomas Fiorido [c], João V. N. de Palma [a], Waldir Avansi Jr [a], Khalifa Aguir [c], Marc Bendahan [c]

[a] Laboratory of Nanostructured Multifunctional Materials, Department of Physics, Federal University of São Carlos, 13565-905, São Carlos, SP, Brazil
[b] Center for the Development of Functional Materials, Federal University of São Carlos, 13565-905, São Carlos, SP, Brazil
[c] Aix Marseille Univ, Université de Toulon, CNRS, IM2NP, Marseille, France

ARTICLE INFO

Keywords:
Fe_2O_3
Hematite
Gas sensor
BTEX
Benzene
Toluene
Ethylbenzene
Xylenes

ABSTRACT

Over the past fifty years, gas sensors based on metal semiconducting oxides (MOXs) have drawn attention due to their performance in detecting various gases. Thus, we report herein on a BTEX gases sensor based on hematite (α-Fe_2O_3) microrhombuses synthesized via the hydrothermal method. X-ray diffraction and X-ray absorption spectroscopy analyses indicated the presence of a pristine hematite phase after hydrothermal treatment. Electron microscopy analyses revealed that the hematite sample consists of single-crystals with a rhombus-like shape and an average size of 140 nm. Electrical measurements pointed out that hematite microrhombuses were sensitive towards sub-ppm BTEX levels, in which the minimum detected level was 3 ppb and the long-term stability was 1 month. The results presented here demonstrate the potential of hematite microrhombuses as a sensing material to manufacture BTEX gas sensor devices.

1. Introduction

The development in industrial and agricultural activities, mainly in developing countries, has resulted in the enhancement of harmful gases dumped into the atmosphere, such as CO, NO, H_2S, NO_2, O_3, and Volatile Organic Compounds (VOCs) [1–6]. The presence of these gases could cause adverse effects on the climate and human life. According to the World Health Organization (WHO), these chemical species may cause serious diseases (e.g. heart and lung diseases, stroke, cancer and acute respiratory infections) or in severe cases, death [6–9]. It is estimated that air pollution has been responsible for the death of 7 million people worldwide every year [6]. Furthermore, approximately 80 % of the urban population is exposed (indoors and outdoors) towards pollution levels that exceed the guidelines recommended by health organizations [3,6,10]. Note that adequate levels of air pollution would also provide a lower demand for hospital admissions (or care), since hospitalizations would decrease [7]. Therefore, the continuous and efficient monitoring of atmospheric gas pollutants is essential.

Among the dangerous gases, BTEX (Benzene, Toluene, Ethylbenzene, and the three Xylene isomers) gases belong to the aromatic VOCs group [11–15]. The main sources for BTEX emissions are indoor and outdoor, such as gas stations, fuel storage, road traffic, and also household products, such as paints, solvents, waxes, pesticides, among others [11–14]. Various investigations have focused on BTEX gases due to their toxic, mutagenic, and/or carcinogenic effects [8,12,16–18]. According to the OSHA (Occupational Safety and Health Administration), the permissible employee exposure to BTEX gases is an average concentration of 0.5 ppm (parts-per-million) for benzene, 200 ppm for toluene and 100 ppm for ethylbenzene and xylene [12].

Generally, BTEX gases have been identified and quantified using gas chromatography [11,17]. However, this equipment, besides being expensive, is not portable, making in-situ analyses difficult [13]. Thus, several investigations have focused on the development of portable devices that allow efficient detection and monitoring of BTEX gases in indoor and outdoor environments.

In past decades, MOXs have been widely used in resistive-type gas sensors to detect (non-) toxic gases. Their main advantages are the low cost, small size, high sensitivity and stability, fast response/recovery and portability [4,19–21]. MOXs have also been used as sensing layers for detecting BTEX gases, such as WO_3, ZnO, and MoO_3 [12,14,22,23], as well as some heterojunctions, for example, SnO_2/V_2O_5, and CuO/SnO_2 [24,25].

Hematite (α-Fe_2O_3) is an n-type wide band-gap semiconductor (E_g = 2.1 eV, at 300 K) [26]. It is the most abundant and the cheapest MOX obtained in the Earth'crust [27], exhibiting potential applications in photocatalysis, energy generation, and lithium batteries [2,26–32]. The

* Corresponding author.
E-mail address: lfsilva83@gmail.com (L.F. da Silva).

https://doi.org/10.1016/j.snb.2020.128817
Received 7 April 2020; Received in revised form 8 July 2020; Accepted 26 August 2020
Available online 2 September 2020

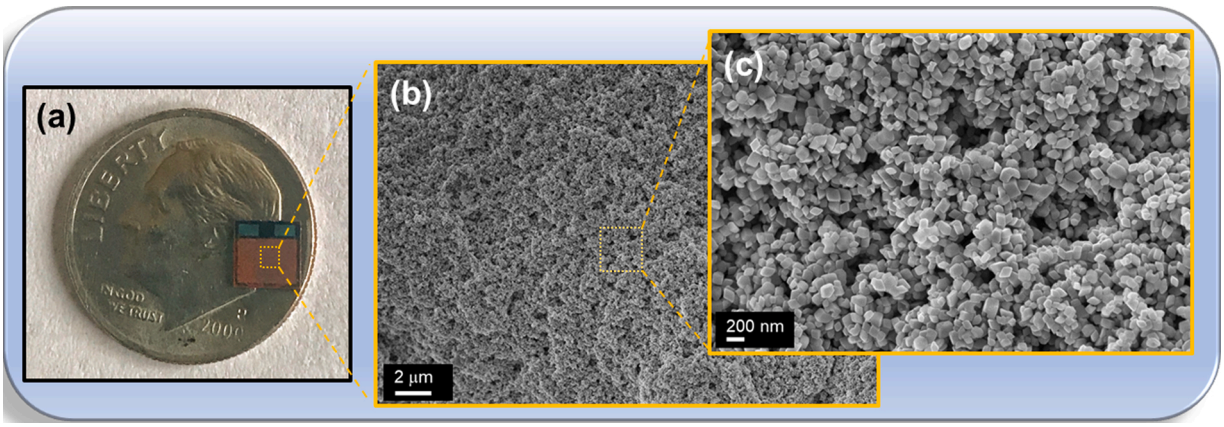

Fig. 1. (a) Photography of sensing platform based on hematite microcrystals compared to a U.S quarter-dollar coin. (b)-(c) FE-SEM images show the homogeneity of the thick film.

Fe_2O_3 compound has also been studied as sensing layer for detection of a wide range of analytes [33–38]. For example, Tian and co-workers reported that hematite nanoboxes obtained via metal-organic framework method were highly sensitive to H_2S gas at an optimum temperature of 200 °C, besides exhibiting a good selectivity towards NO, CO and NH_3 gases [38]. Despite the remarkable gas-sensing properties of hematite, few researchers have studied its performance in relation to the detection of BTEX gases. Kim and co-workers prepared vertically hematite nanotubes applied as a gas-sensing layer. They observed a high response towards acetone compared to other analytes (benzene, toluene, acetone, ethanol and CO) at an operating temperature relatively high equal to 350 °C [27]. Also, Thu and co-workers reported good selectivity and sensitivity to ethanol of a hematite nanoporous sample working at 400 °C. In a similar work, Park and co-workers observed in hematite microcubes a high sensitivity to VOCs, especially formaldehyde, at an operating temperature of 300 °C [31].

Motivated by these arguments, we report herein a versatile and efficient approach to obtain hematite microcrystals presenting remarkable properties for application as a BTEX gases-sensing layer. The microcrystals were synthesized via the hydrothermal method and characterized by X-ray diffraction (XRD), field-emission scanning electron (FE-SEM) and high-resolution transmission electron microscopies (HR-TEM), and X-ray absorption near-edge structure (XANES) spectroscopy. The α-Fe_2O_3 microcrystals were studied in relation to the detection of BTEX, acetone, and ethanol. Electrical measurements revealed their higher sensitivity to sub-ppm BTEX levels compared to other VOCs. These results have a significant impact on the scientific field due to their practical potential for environmental monitoring applications.

2. Experimental section

2.1. Preparation of microcrystals

The α-Fe_2O_3 microcrystals were obtained by the hydrolysis of iron (III) chloride hexahydrate ($FeCl_3.6H_2O$, 99.9 %, Sigma-Aldrich) in ethyl

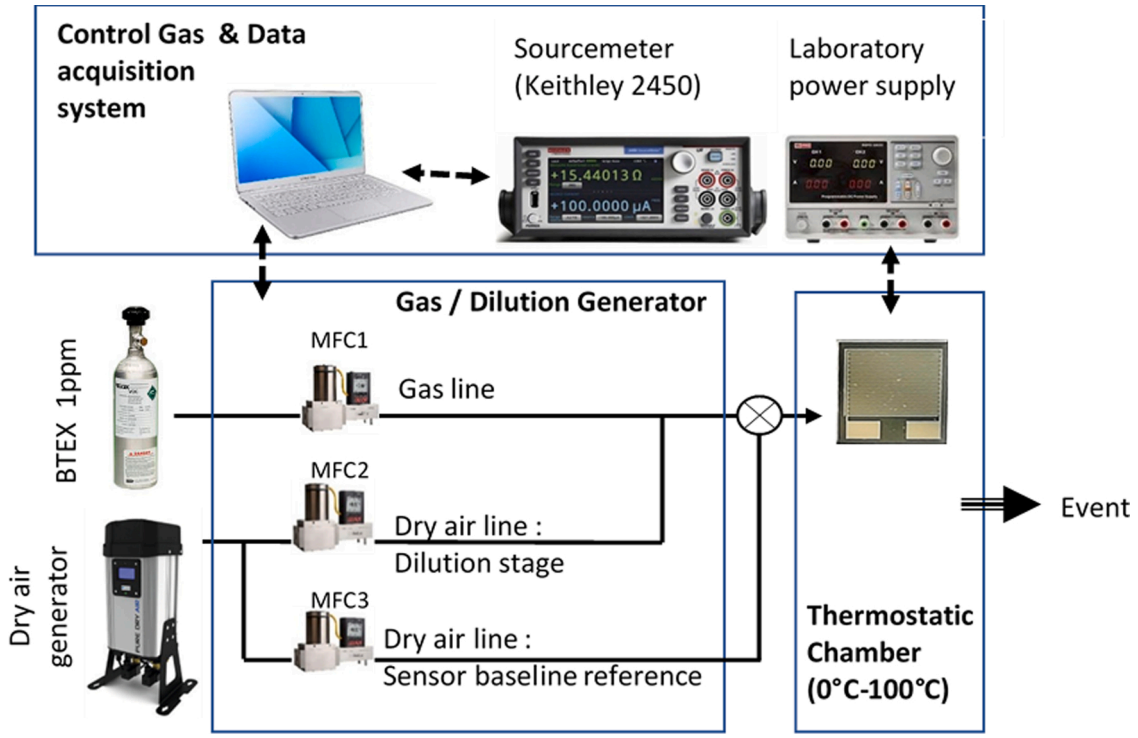

Fig. 2. Experimental workbench used in the gas-sensing experiments of BTEX gases.

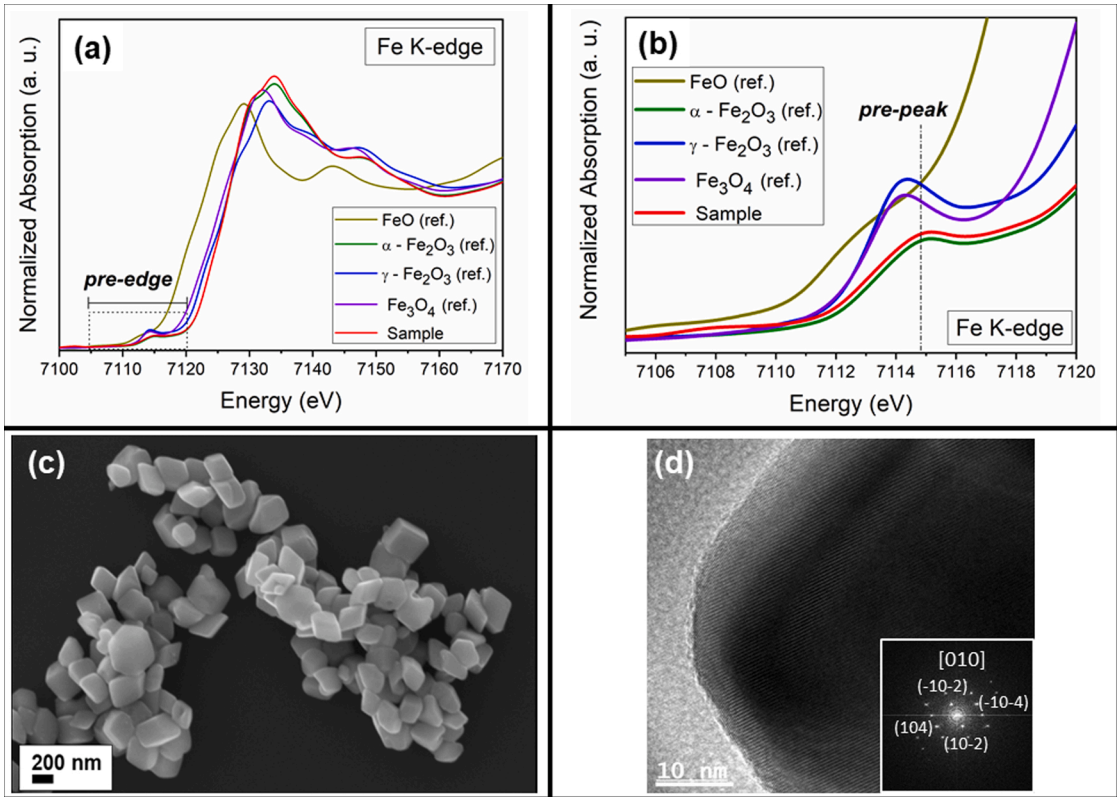

Fig. 3. The as-prepared α-Fe_2O_3 microcrystals prepared via hydrothermal treatment. (a) Fe K-edge XANES spectra. (b) Details of the pre-edge XANES region. For the sake of comparison, the iron oxide reference compounds (FeO, α-Fe_2O_3, γ-Fe_2O_3 and Fe_3O_4) were added. (c) FE-SEM and (d) HR-TEM micrographs. The respective Fourier Transform (FT) of HRTEM images is presented in the inset of Fig. 3(d).

alcohol anhydrous at room temperature. The concentration of iron chloride diluted in alcohol was 0.06 M. Afterwards, deionized water was slowly added to the reactional solution to obtain a molar ratio of Fe(III) : H_2O = 1:500. The chloride anions were removed by the dialysis process, and the precipitate was then dried in an electric oven during 12 h at 80 °C. To obtain the hematite phase, the precipitate powder was diluted in deionized water (1 g L^{-1}) and then submitted to hydrothermal treatment for 4 h at 200 °C with a heating rate of 2 °C min^{-1}. The precipitated powders were washed with deionized water and isopropyl alcohol and dried at 80 °C overnight under the air atmosphere.

2.2. Characterization techniques

X-ray diffraction (XRD) measurements were carried out using CuK_α radiation (Rigaku diffractometer, model D/Max-2500PC) in a 2θ range from 20° to 80° with a step of 0.02° at a scanning speed of 2° min^{-1}. The morphological properties were investigated using a field emission scanning electron microscopy (FE-SEM, Zeiss Supra35) and a transmission electron microscopy (TEM, FEI Tecnai G2 F20) operated at 200 KeV. The mean particle size was estimated by analyzing FE-SEM micrographs through the measure of approximately 100 particles. X-ray absorption spectroscopy (XAS) experiments were carried out in the D08B-XAFS2 beamline at the Brazilian Synchrotron Light Laboratory (LNLS). The experiments were carried out at the Fe K-edge (7112 eV) in a transmission mode at room temperature using a flat Si(111) double crystal monochromator. X-ray absorption near-edge structure (XANES) spectra were collected for each sample between 7090 and 7190 eV using energy steps of 0.5 eV. For the sake of comparison, all spectra were background removed and normalized using as unity the first EXAFS (Extended X-ray Absorption Fine Structure) oscillation using MAX software [39].

2.3. Gas-sensing experiments

Hematite microcrystals were dispersed in isopropyl alcohol (20 mg mL^{-1}) using an ultrasonic cleaner for 30 min and then the suspension was dropped three times onto a Si/SiO_2 substrate containing 100 nm thick Pt interdigitated electrodes separated by a distance of 50 μm. After deposition, the sensor was then treated at 500 °C in an electric oven under the air atmosphere for 1 h at a heating rate of 10 °C min^{-1}. The photography of the sensing platform and FE-SEM images of the hematite microcrystals used in the experiments are presented in Fig. 1.

The gas-sensing experiments were carried out in a dynamic chamber that allows us to control the operating temperature and to obtain various gas concentrations by using Mass Flow Controllers (MFC) [12]. This workbench, Fig. 2, can produce low BTEX concentrations from 1 to 400 ppb (part-per-billion) from the dilution with dry air. The total gas flow rate was kept constant and equal to 500 SCCM. The workbench also allows the control of relative humidity (% RH) from 0 to 90 %. The cylinder containing the mixture of BTEX gases was purchased from Air Liquide company (France). The concentration of each component in the BTEX mixture is displayed in Table S1. Further details regarding the gas-sensing workbench may be found in previous work in Ref. [12]. The applied DC voltage was kept constant, while the electrical resistance was monitored using an electrometer (Keithley, model 2540). The sensor response (S) was defined as $S(\%) = ((R_{air} - R_{BTEX})/R_{air}).100$, where R_{air} and R_{BTEX} are the electrical resistances of the sensor upon exposure to dry air and BTEX gases, respectively. The response and recovery times were estimated following the procedure reported elsewhere [3,4,20].

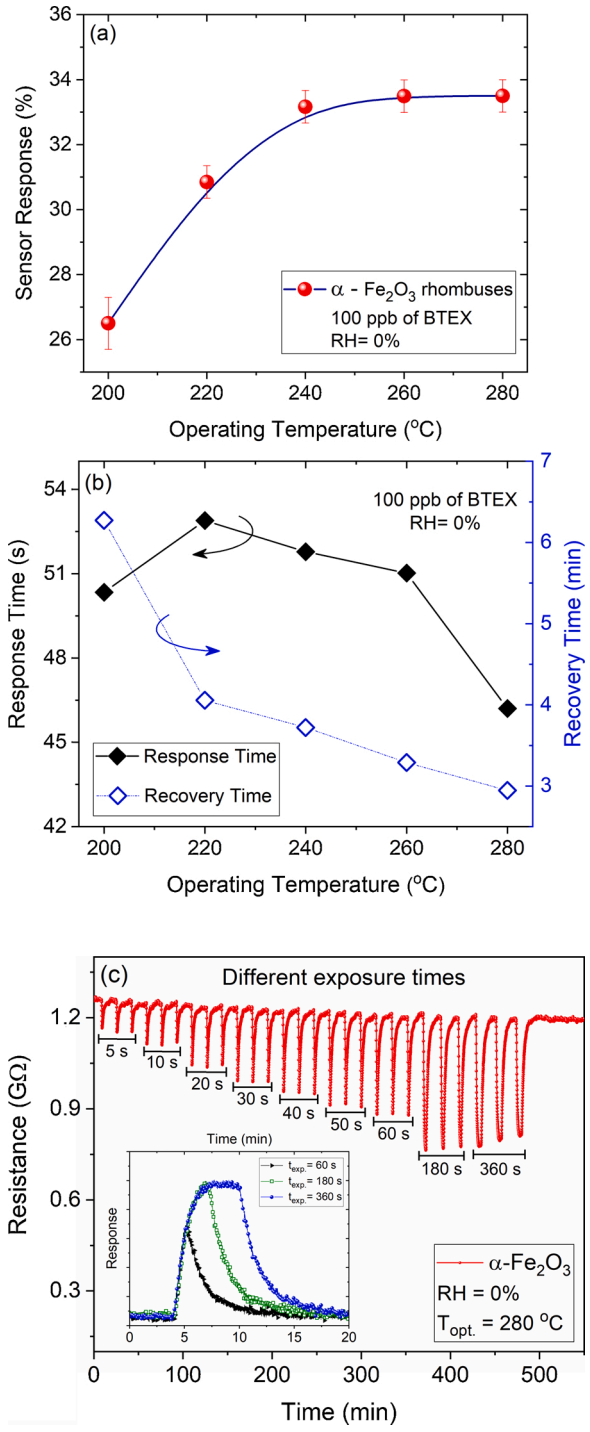

Fig. 4. (a) Gas-sensing performance of α-Fe_2O_3 microrhombuses exposed towards 100 ppb of BTEX gases, and (b) variation of response and recovery times at operating temperatures between 200 and 280 °C. (c) Electrical resistance of the microrhombuses exposed to BTEX gases during different time intervals. The inset shows the evolution of sensor response with exposure time.

3. Results and discussion

3.1. Microstructural properties

X-ray diffraction pattern of the as-synthesized sample prepared via the hydrothermal route is shown in Fig. S1(a). All reflections were indexed to a pristine rhombohedral hematite (α-Fe_2O_3) phase with an R3c space group (JCPDS file 87-1164). Fe K-edge spectra of iron-oxide based compounds and the as-prepared hematite sample are displayed in Fig. 3(a) and (b). The comparison of reference compound spectra with the sample confirms the presence of the pristine α-Fe_2O_3 phase, with iron atoms in octahedral coordination, FeO_6 [30].

FE-SEM image in Fig. 3(c) reveals homogeneity in the morphology of the as-studied microcrystals, exhibiting a well-defined rhombus-like shape with an average size of approximately 140 nm. The HRTEM image of a selected region of an individual crystal and its respective Fourier Transform (FT), Fig. 3(d), shows the monocrystalline nature of the as-studied sample.

3.2. BTEX sensing performances

The gas-sensing performances of α-Fe_2O_3 microrhombuses were evaluated towards BTEX gases. Initially, the optimum operating temperature of the sample was evaluated by exposing it to 100 ppb of analyte and varying only the operating temperature, as seen in Fig. 4. The electrical measurements carried out at different working temperatures are presented in Fig. S2. For temperatures below 200 °C, no sensitivity towards BTEX gases was observed.

The highest sample responses were achieved in the temperature range of 240–280 °C, as shown in Fig. 4(a). In addition, the behavior of response and recovery times as a function of operating temperature is displayed in Fig. 4(b). We can observe that despite the fact that the sample required a long time for the complete desorption of BTEX molecules, its response time was relatively fast (at around 50 s). In addition, when the sample was exposed to 100 ppb of BTEX during different time intervals (from 5 s to 360 s), Fig. 4(c), it was possible to observe that it was sensitive to BTEX gases at various exposure times, mainly the shortest one (5 s), while, the sample saturation level was reached at exposure times longer than 180 s, as illustrated in the inset of Fig. 4(c). It is interesting to note that even after a long sequence of exposure cycles (> 8 h) the sample exhibited a total recovery, indicating that its surface was not damaged.

To obtain short recovery times of the sensing material, we chose 280 °C as the optimum working temperature for further experiments. Thus,The hematite microrhombuses were kept at 280 °C and then exposed to several different BTEX levels, from 3 to 400 ppb. It should be mentioned that for gas levels lower than 3 ppb, the microcrystals did not exhibit any sensitivity; considering here the above-mentioned temperature.

Fig. 5 shows that the electrical resistance of the microrhombuses decreased during exposition to BTEX gases. When an n-type MOX, such as hematite, is exposed to a reducing gas (e.g. BTEX), the ionized oxygen anions adsorbed at the surface sample oxidize the analyte. During this adsorption process, the release of the electrons occurs from the MOX surface, consequently decreasing the electrical resistance of the sensing material [5,35,40,41].

Regarding the sensor responses, the hematite microcrystals showed good sensitivity even for very low BTEX levels, in addition to complete recovery after each exposure cycle. The sample also exhibited high repeatability of its response, reinforcing its reliability, as demonstrated by the seven exposure cycles displayed in Fig. 5(d).

Fig. 6 displays the sensor response of α-Fe_2O_3 microrhombuses, kept at 280 °C and, exposed towards different BTEX levels, from 3 to 400 ppb. The response enhancement as a function of the BTEX level is clear, with no evidence of saturation in the evaluated range. Despite the fact that the microcrystals had detected sub-ppm gas levels, the inset of Fig. 6 shows that the response had a low variation between 3 and 10 ppb, meaning a low accuracy in this range. Nevertheless, this finding does not debunk the hematite for practical applications, as long as just BTEX levels above 500 ppb become harmful to human health, as recommended by the WHO.

Regarding the sensor response behaviors with BTEX levels, an exponential trend in the sensor response of hematite microrhombuses was obtained. It is well established that the sensor response (S) of MOXs

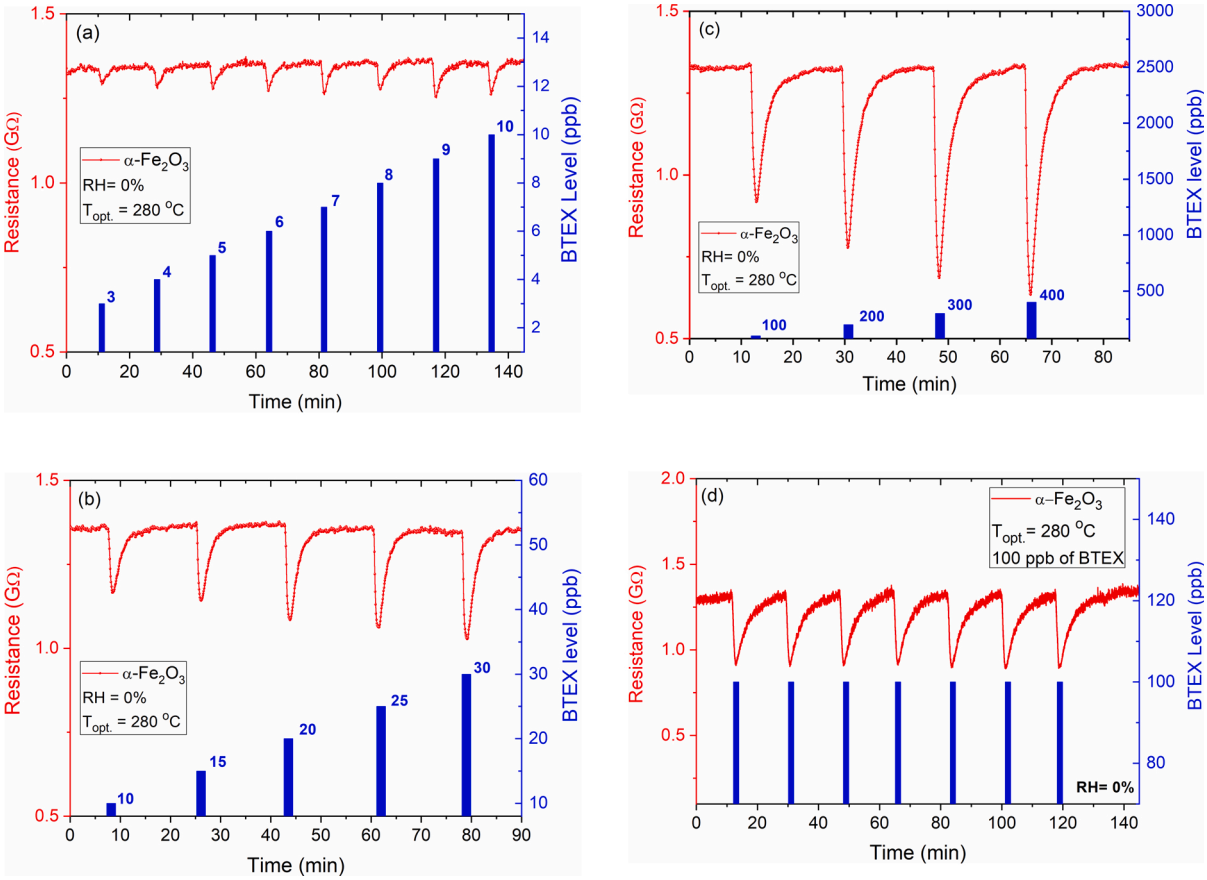

Fig. 5. Gas-sensing response of the α-Fe_2O_3 microrhombuses kept at 280 °C and exposed to different BTEX levels: (a) 3 to 10 ppb, (b) 10 to 30 ppb, and (c) 100 to 400 ppb. (d) Sensor response for seven exposure cycles of 100 ppb of BTEX gases.

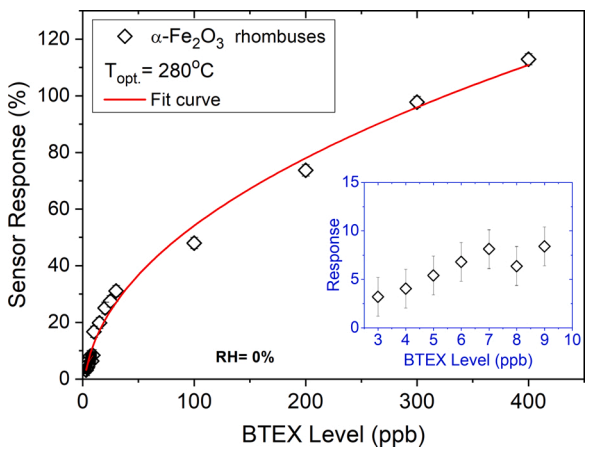

Fig. 6. Sensor response of the α-Fe_2O_3 microrhombuses *vs.* BTEX level. The inset shows the response variation for a BTEX level between 3 and 10 ppb.

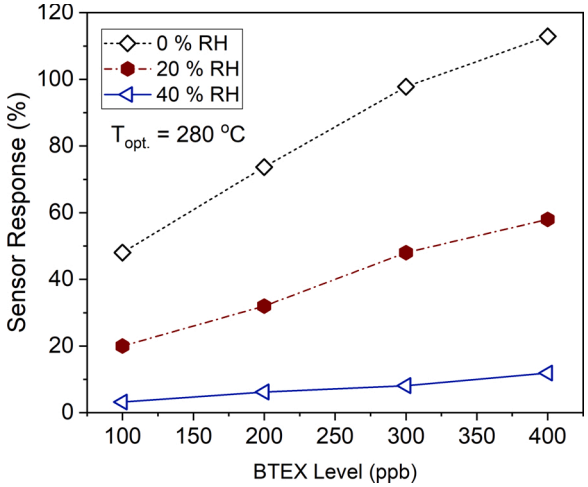

Fig. 7. Sensor response of the α-Fe_2O_3 microrhombuses *vs.* BTEX level under different relative humidity (% RH) values at an operating temperature of 280 °C.

complies with the following power-law equation: $S(C) = A(C)^n$, where A is a constant, *n* the exponent, and *C* is the concentration of the investigated analyte [42]. Herein, the best fitting law acquired from the experimental data was found to be the equation: $S(C) = 7.617.(C)^{0.461}$.

The influence of relative humidity on the BTEX gas sensing performance was also investigated. To this end, the sample was kept at 280 °C and then exposed to 100, 200, 300, and 400 ppb of BTEX gases under different relative humidity (0, 20, and 40 % RH) values. It can be seen that the BTEX sensor response was reduced by the presence of water molecules, as shown in Fig. 7. This behavior is due to the competition of water and BTEX molecules by actives sites on the sample surface, impairing the detection of BTEX molecules. Zhang and co-workers reported similar humidity effect for WO_3 nanosheets used as sensing material to detect BTEX (Benzene, Toluene, Ethylbenzene, and p-Xylol) vapors [14].

Gas selectivity and long-term stability are desirable characteristics in the development of gas sensor devices. Fig. 8(a) illustrates the response (S) of the microrhombuses exposed to BTEX gases, ethanol, and acetone

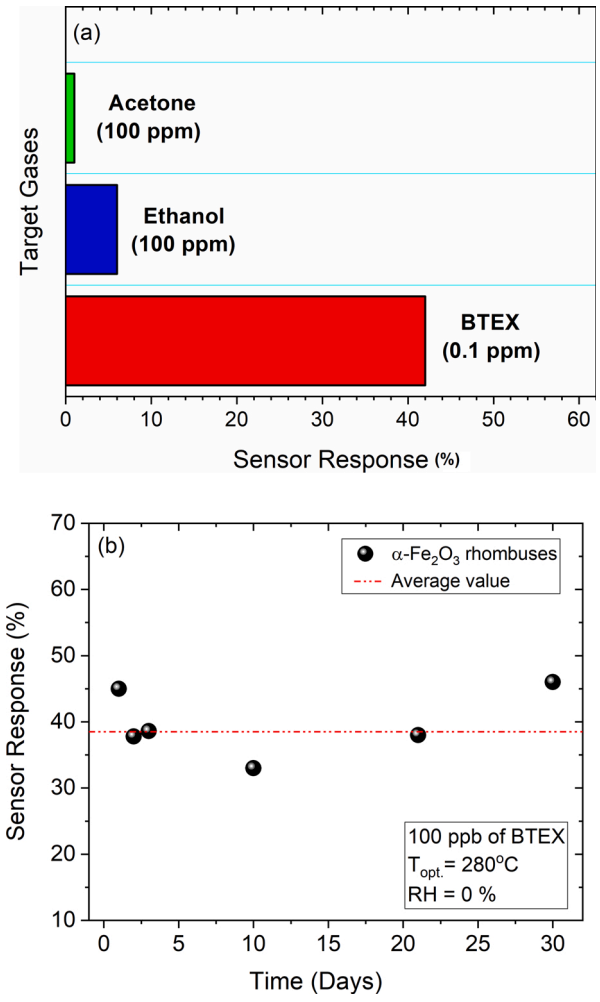

Fig. 8. Sensor performance of α-Fe_2O_3 microrhombuses at 280 °C. (a) Comparison of the response for an exposure of 0.1 ppm of BTEX gases, 100 ppm of acetone, and 100 ppm of ethanol. (b) Response of the sample upon exposure to 100 ppb of BTEX gases for 30 days.

Table 1
Gas-sensing performance of the MOXs used as a BTEX sensing material.

Sensing material	Processing method	$T_{opt.}$ (°C)	BTEX level* (ppb)	Reference
m - WO_3	RF-sputtering	260	5	12
h - WO_3	Hydrothermal	320	1000	14
Au - ZnO	Hydrothermal	206	1000	43
Au -MoO_3	Solvothermal	250	100	23
CuO / SnO_2	Microwave-assisted	280	2000	24
SnO_2 / V_2O_5	Sol-gel	270	500	25
α - Fe_2O_3	Hydrothermal	240 - 280	3	Our work

* Minimum BTEX level, experimentally, detected.

gases at 280 °C. Notably, the hematite microrhombuses exhibited a higher response to BTEX gases compared to the investigated VOCs gases. Regarding the long-term stability, it was evaluated by exposing the microrhombuses towards 100 ppb of BTEX gases for 30 days, and the results are presented in Fig. 8(b). It can be noted after the mentioned period that the sample still detected a very low BTEX level. It means that the lifetime of the hematite microrhombuses can be superior to 1 month since the sample surface was not poisoned/damaged as a result of the several exposures to BTEX gases.

Table 1 shows the performance of some MOXs synthesized by different methodologies, applied as a BTEX gases sensing material. As seen, the range of working temperatures of such MOXs is similar to those found here for the microrhombuses. Nevertheless, we must draw attention to the sensitivity of hematite microrhombus that detected a very low BTEX level, i.e., 3 ppb. Based on the findings presented here, it is reasonable to consider the potential of hematite microcrystals as a sensing material for BTEX sensors.

3.3. Gas-sensing mechanism

We propose herein a possible sensing mechanism of the hematite microrhombuses to detect BTEX, i.e., Benzene (C_6H_6), Toluene ($C_6H_5CH_3$), Ethylbenzene (C_8H_{10}) and Xylene ($C_6H_4(CH_3)_2$) gases. According to the literature, for resistive-type gas sensors, the sensing mechanism is based on the adsorption process of the oxygens and the target gas molecules which occurs on the MOX surface, depending on the sensing material characteristics (e.g. particles size, and morphology), working temperature, analyte concentration, environmental conditions (e.g. pressure and humidity), etc. [41,44–48].

Regarding the hematite microrhombuses, when the oxygen molecules are adsorbed on the sample surface, they trap free electrons from the hematite conduction band. This ionosorption process increases the band bending (qV_s), forming a depletion region "d" on the hematite microrhombuses surface, as illustrated in Fig. 9(a) and (b). At operating temperatures higher than 280 °C, the ionic O^- species are dominant [5,13,46]. This process can be expressed by:

$$O_{2(ads)} + 2e^- \rightarrow 2O^-_{(ads)} \quad (1)$$

Upon exposure to a reducing gas, such as BTEX gases, the electrical resistance of the hematite decreases due to the reaction between the molecules of the reducing gas and the ionosorberd oxygens (O^-) at the rhombus surface, releasing the electrons to the conduction band. This behavior reduces the height of potential barrier qV_s, consequently decreasing the depletion region "d" and enhancing the conductivity of the hematite microrhombuses [43–45,49]. Fig. 9(b) illustrates the possible sensing mechanism of hematite microrhombuses to detect BTEX gases. In this figure, it is suggested that the possible sub-products formed by the interaction between the BTEX gases and the sample surface are H_2O and CO_2.

4. Conclusion

In summary, we report here the synthesis of hematite microcrystals via hydrothermal route for use as BTEX gases-sensing material. XRD pattern and Fe K-edge XANES spectra revealed the presence of the pristine hematite phase. The FE-SEM and HR-TEM analyses showed that the hematite microcrystals exhibit a well-defined rhombus-like shape with a single-crystal nature. Electrical measurements showed a good sensitivity towards BTEX gases at an operating temperature of 280 °C. The microrhombuses detected the lowest gas levels that ranged from 3 ppb to 400 ppb, exhibiting excellent repeatability and stability, and good selectivity towards acetone and ethanol. Finally, our findings highlighted the promising properties of hematite microrhombuses as BTEX gas sensors for practical applications.

Author contributions

The manuscript was written through the contributions of all authors. All authors have approved the final version of the manuscript.

CRediT authorship contribution statement

Luís F. da Silva: Conceptualization, Methodology, Data curation, Writing - original draft, Investigation, Writing - review & editing. **Ariadne C. Catto:** Investigation, Methodology, Writing - review & editing. **Sandrine Bernardini:** Data curation, Writing - review & editing. **Tomas Fiorido:** Investigation, Writing - review & editing. **João V. N. de Palma:** Methodology, Data curation, Writing - review & editing.

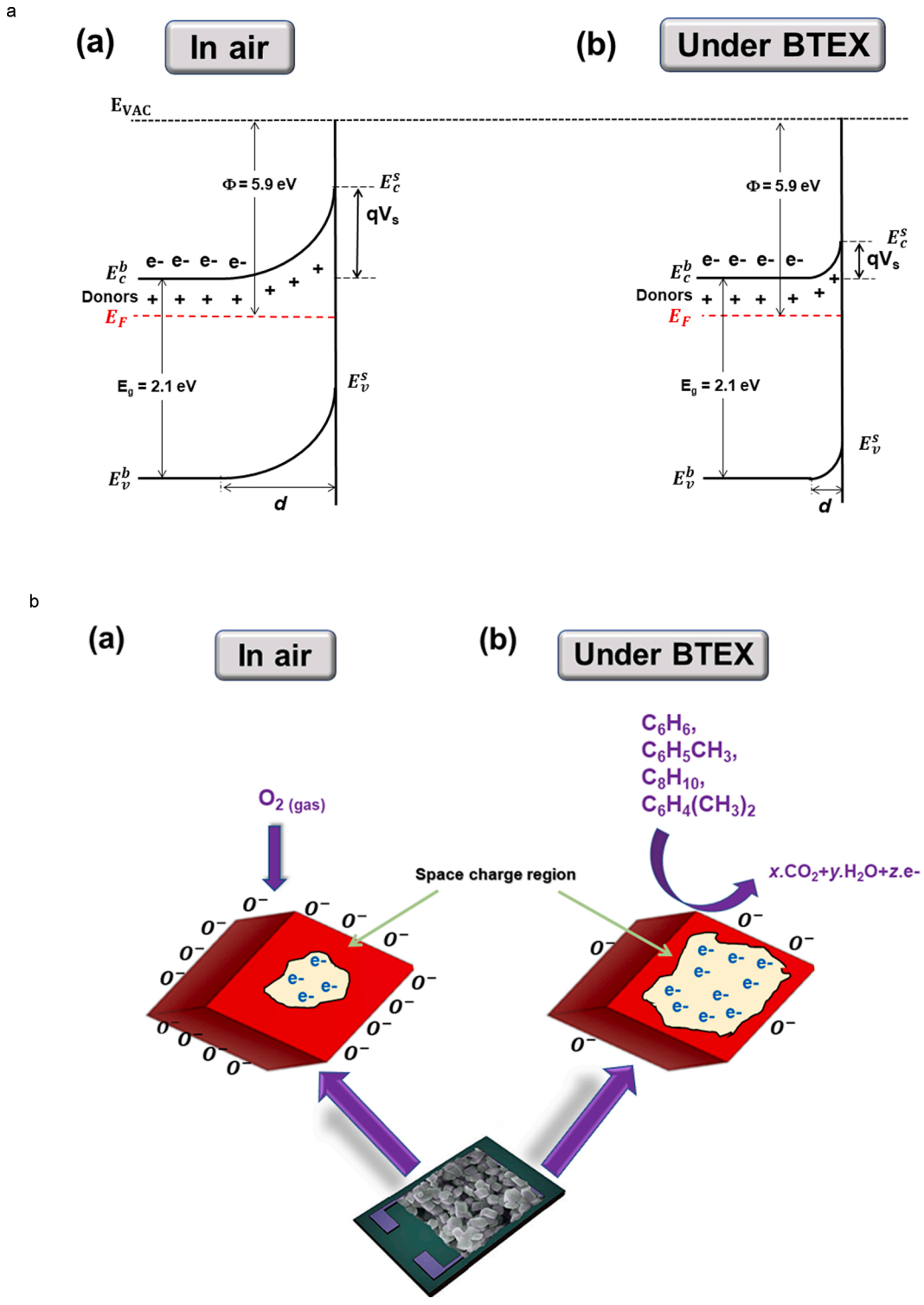

Fig. 9. Schematic illustration of the sensing mechanism of hematite rhombus-like crystals to detect BTEX gases. (a) Under air atmosphere, and (b) exposure to BTEX gases.

Waldir Avansi: Data curation, Writing - original draft, Writing - review & editing. **Khalifa Aguir:** Supervision, Writing - review & editing. **Marc Bendahan:** Investigation, Methodology, Data curation, Supervision, Writing - review & editing.

Declaration of Competing Interest

The authors report no declarations of interest.

Acknowledgments

The authors thank Dr. Julio C. Sczancoski for the XRD data and Mr. Rorivaldo Camargo, who operated the FE-SEM microscope. This investigation was initiated at the Institute of Material and Microelectronics of Provence (France) during a period of visiting professor at the Aix-Marseille University. This research was also partially performed at the Brazilian Nanotechnology National Laboratory (Microfabrication team:

Project LMF-18580), and the Brazilian Laboratory of Synchrotron Radiation (LNLS, Project D04B-XAFS2-20180311), Campinas, SP, Brazil. We also thank the Laboratory of Structural Characterization (LCE/DEMa/UFSCar) for the TEM facilities. The authors acknowledge the financial support of the Brazilian research funding institutions: FAPESP (under grants No. 2017/12437-5, 2019/18082-2, 2018/18208-0 and 2013/07296-2), CNPq (under grants No. 405140/2018-5, 426511/2018-2, 308706/2018-8, and 311463/2017-7) and CAPES.

Appendix A. Supplementary data

Supplementary material related to this article can be found, in the online version, at doi:https://doi.org/10.1016/j.snb.2020.128817.

References

[1] P.M. Lemieux, C.C. Lutes, D.A. Santoianni, Emissions of organic air toxics from open burning: a comprehensive review, Prog. Energy Combust. Sci. 30 (2004) 1–32.
[2] A. Mirzaei, B. Hashemi, K. Janghorban, α-Fe_2O_3 based nanomaterials as gas sensors, J. Mater. Sci. Mater. Electron. 27 (2016) 3109–3144.
[3] A.C. Catto, L.F. da Silva, M.I.B. Bernardi, S. Bernardini, K. Aguir, E. Longo, V. R. Mastelaro, Local structure and surface properties of $Co_xZn_{1-x}O$ thin films for ozone gas sensing, ACS Appl. Mater. Interfaces 8 (2016) 26066–26072.
[4] W. Avansi Jr, A.C. Catto, L.F. da Silva, T. Fiorido, S. Bernardini, V.R. Mastelaro, K. Aguir, R. Arenal, One-dimensional $V2O_5$/TiO2 heterostructures for chemiresistive ozone sensors, ACS Appl. Nano Mater. 2 (2019) 4756–4764.
[5] H.-J. Kim, J.-H. Lee, Highly sensitive and selective gas sensors using p-type oxide semiconductors: overview, Sens. Actuators, B 192 (2014) 607–627.
[6] World Health Organization - WHO/Health Topics/ Air Pollution. (Accessed in 28 February 2020), https://www.who.int/health-topics/air-pollution#tab=tab_1.
[7] C.K. Abe, G.S. Miraglia, Health impact assessment of air pollution in São Paulo, Brazil, Int. J. Environ. Res. Public Heal. 13 (2016) E694.
[8] M. Kampa, E. Castanas, Human health effects of air pollution, Environ. Pollut. 151 (2008) 362–367.
[9] S.-Y. Lin, S.-W. Ju, C.L. Lin, W.-H. Hsu, C.-C. Lin, I.-W. Ting, C.-H. Kao, Air pollutants and subsequent risk of chronic kidney disease and end-stage renal disease: a population-based cohort study, Environ. Pollut. 261 (2020) 114154.
[10] S. Saksena, P.B. Singh, R.K. Prasad, R. Prasad, P. Malhotra, V. Joshi, R.S. Patil, Exposure of infants to outdoor and indoor air pollution in low-income urban areas - a case study of Delhi, J. Expo. Sci. Environ. Epidemiol. 13 (2003) 219–230.
[11] I. Lara-lbeas, A. Rodríguez-Cuevas, C. Andrikopoulou, V. Person, L. Baldas, S. Colin, S. Le Calvé, Sub-ppb level detection of BTEX gaseous mixtures with a compact prototype GC equipped with a preconcentration unit, Micromachines 10 (2019) 187.
[12] A. Favard, K. Aguir, T. Contaret, A. Dumas, M. Bendahan, Detection and measuring of BTEX traces at the ppb level using metal oxide gas sensor, Mater. Today Proc. 6 (2019) 323–327.
[13] A. Mirzaei, J.-H. Kim, H.W. Kim, S.S. Kim, Resistive-based gas sensors for detection of benzene, toluene and xylene (BTX) gases: a Review, J. Mater. Chem. C 6 (2018) 4342–4370.
[14] D. Zhang, Y. Fan, G. Li, Z. Ma, X. Wang, Z. Cheng, J. Xu, Highly sensitive BTEX sensors based on hexagonal WO_3 nanosheets, Sens. Actuators, B 293 (2019) 23–30.
[15] A. Allouch, S. Le Calvé, C.A. Serra, Portable, miniature, fast and high sensitive real-time analyzers: BTEX detection, Sens. Actuators, B 182 (2013) 446–452.
[16] R. Duarte-Davidson, C. Courage, L. Rushton, L. Levy, Benzene in the environment: an assessment of the potential risks to the health of the population, Occup. Environ. Med. 58 (2001) 2–13.
[17] A. Rafiee, J.M. Delgado-Saborit, P.D. Sly, H. Amiri, M. Hoseini, Lifestyle and occupational factors affecting exposure to BTEX in municipal solid waste composting facility workers, Sci. Total Environ. 656 (2019) 540–546.
[18] S.M. Correa, G. Arbilla, M.R.C. Marques, K.M.P.G. Oliveira, The impact of BTEX emissions from gas stations into the atmosphere, Atmos. Pollut. Res. 3 (2012) 163–169.
[19] N. Barsan, D. Koziej, U. Weimar, Metal oxide-based gas sensor research: How to? Sens. Actuators, B 121 (2007) 18–35.
[20] L.F. da Silva, A.C. Catto, W. Avansi Jr, L.S. Cavalcante, J. Andres, K. Aguir, V. R. Mastelaro, E. Longo, A novel ozone gas sensor based on one-dimensional (1D) α-Ag_2WO_4 nanostructures, Nanoscale 6 (2014) 4058–4062.
[21] L.F. da Silva, J.-C. M'Peko, A.C. Catto, S. Bernardini, V.R. Mastelaro, K. Aguir, C. Ribeiro, E. Longo, UV-enhanced ozone gas sensing response of ZnO-SnO_2 heterojunctions at room-temperature, Sens. Actuators, B 240 (2017) 573–579.
[22] S.P. Choudhury, Z. Feng, C. Gao, X. Ma, J. Zhan, F. Jia, BN quantum dots decorated ZnO nanoplates sensor for enhanced detection of BTEX gases, J. Alloys. Compd. 815 (2020), 152376.
[23] L. Sui, X. Zhang, X. Cheng, P. Wang, Y. Xu, S. Gao, H. Zhao, L. Huo, Au-loaded hierarchical MoO_3 hollow spheres with enhanced gas-sensing performance for the detection of BTX (benzene, toluene, and xylene) and the sensing mechanism, ACS Appl. Mater. Interfaces 9 (2017) 1661–1670.
[24] F. Ren, L. Gao, Y. Yuan, Y. Zhang, A. Alqrni, O.M. Al-Dossary, J. Xu, Enhanced BTEX gas-sensing performance of CuO/SnO_2 composite, Sens. Actuators, B 223 (2016) 914–920.
[25] F. Zhang, X. Wang, J. Dong, N. Qin, J. Xu, Selective BTEX sensor based on a SnO_2/V_2O_5 composite, Sens. Actuators, B 186 (2013) 126–131.
[26] G. Bailly, J. Rossignol, B. de Fonseca, P. Pribetich, D. Stuerga, Microwave gas sensing with hematite: shape effect on ammonia detection using pseudocubic, rhombohedral, and spindlelike particles, ACS Sens. 1 (2016) 656–662.
[27] D.H. Kim, Y.-S. Shim, J.-M. Jeon, H.Y. Jeong, S.S. Park, Y.-W. Kim, J.-S. Kim, J.-H. Lee, H.W. Jang, Vertically ordered hematite nanotube array as an ultrasensitive and rapid response Acetone Sensor, ACS Appl. Mater. Interfaces 6 (2014) 14779–14784.
[28] N.D. Cuong, T.T. Hoa, D.Q. Khieu, N.D. Hoa, N. Van Hieu, Gas sensor based on nanoporous hematite nanoparticles: effect of synthesis pathways on morphology and gas sensing properties, Curr. Appl. Phys. 12 (2012) 1355–1360.
[29] J. García-Serrano, E. Gómez-Hernández, M. Ocampo-Fernández, U. Pal, Effect of Ag doping on the crystallization and phase transition of TiO_2 nanoparticles, Curr. Appl. Phys. 9 (2009) 1097–1105.
[30] C. Wu, P. Yin, X. Zhu, C. OuYang, Y. Xie, Synthesis of hematite (α-Fe_2O_3) nanorods: diameter-size and shape effects on their applications in magnetism, lithium ion battery, and gas sensors, J. Phys. Chem. B 110 (2006) 17806–17812.
[31] H.J. Park, S.Y. Hong, D.H. Chun, S.W. Kang, J.C. Park, D.-S. Lee, A highly susceptive mesoporous hematite microcube architecture for sustainable p-type formaldehyde gas sensors, Sens. Actuators, B 287 (2019) 437–444.
[32] T. Ma, L. Zheng, Y. Zhao, Y. Xu, J. Zhang, X. Liu, Highly porous double-shelled hollow hematite nanoparticles for gas sensing, ACS Appl. Nano Mater. 2 (2019) 2347–2357.
[33] M. Debliquy, C. Baroni, A. Boudiba, J.-M. Tulliani, M. Olivier, C. Zhang, Sensing characteristics of hematite and barium oxide doped hematite films towards ozone and nitrogen dioxide, Procedia Eng. 25 (2011) 219–222.
[34] Z. Wu, Z. Li, H. Li, M. Sun, S. Han, C. Cai, W. Shen, Y. Fu, Ultrafast response/recovery and high selectivity of the H_2S gas sensor based on α-Fe_2O_3 nano-ellipsoids from one-step hydrothermal synthesis, ACS Appl. Mater. Interf. 11 (2019) 12761–12769.
[35] D. Peeters, D. Barreca, G. Carraro, E. Comini, A. Gasparotto, C. Maccato, C. Sada, G. Sberveglieri, Au/ε-Fe_2O_3 nanocomposites as selective NO_2 gas sensors, J. Phys. Chem. C 118 (2014) 11813–11819.
[36] V. Balouria, A. Kumar, S. Samanta, A. Singh, A.K. Debnath, A. Mahajan, R.K. Bedi, D.K. Aswal, S.K. Gupta, Nano-crystalline Fe_2O_3 thin films for ppm level detection of H_2S, Sens. Actuators, B 181 (2013) 471–478.
[37] V.V. Malyshev, A.V. Eryshkin, E.A. Koltypin, E.A. Varfolomeev, A.A. Vasiliev, Gas sensitivity of semiconductor Fe_2O_3-based thick-film sensors to CH_4, H_2, NH_3, Sens. Actuators, B 19 (1994) 434–436.
[38] K. Tian, X.X. Wang, Z.Y. Yu, H.Y. Li, X. Guo, Hierarchical and hollow Fe_2O_3 nanoboxes derived from metal–organic frameworks with excellent sensitivity to H_2S, ACS Appl. Mater. Interf. 9 (2017) 29669–29676.
[39] A. Michalowicz, J. Moscovici, D. Muller-Bouvet, K. Provost, MAX: Multiplatform Applications for XAFS, J. Phys. Conf. Ser. 190 (2009) 12034.
[40] D. Flak, A. Braun, B.S. Mun, J.B. Park, M. Parlinska-Wojtan, T. Graule, M. Rekas, Spectroscopic assessment of the role of hydrogen in surface defects, in the electronic structure and transport properties of TiO_2, ZnO and SnO_2 nanoparticles, Phys. Chem. Chem. Phys. 15 (2013) 1417–1430.
[41] C. Malagù, A. Giberti, S. Morandi, C.M. Aldao, Electrical and spectroscopic analysis in nanostructured SnO_2: 'Long-term' resistance drift is due to in-diffusion, J. Appl. Phys. 110 (2011) 93711.
[42] G. Lu, J. Xu, J. Sun, Y. Yu, Y. Zhang, F. Liu, UV-enhanced room temperature NO_2 sensor using ZnO nanorods modified with SnO_2 nanoparticles, Sens. Actuators, B 162 (2012) 82–88.
[43] Z. Shen, X. Zhang, X. Ma, R. Mi, Y. Chen, S. Ruan, The significant improvement for BTX (benzene, toluene and xylene) sensing performance based on Au-decorated hierarchical ZnO porous rose-like architectures, Sens. Actuators, B 262 (2018) 86–94.
[44] K. Suematsu, K. Watanabe, M. Yuasa, T. Kida, K. Shimanoe, Effect of ambient oxygen partial pressure on the hydrogen response of SnO_2 semiconductor gas sensors, J. Electrochem. Soc. 166 (2019) 618–622.
[45] M. Hübner, C.E. Simion, A. Tomescu-Stănoiu, S. Pokhrel, N. Bârsan, U. Weimar, Influence of humidity on CO sensing with p-type CuO thick film gas sensors, Sens. Actuators, B 153 (2011) 347–353.
[46] N. Bârsan, U. Weimar, Understanding the fundamental principles of metal oxide based gas sensors; the example of CO sensing with SnO_2 sensors in the presence of humidity, J. Phys. Condens. Matter 15 (2003) R813.
[47] G. Korotcenkov, B.K. Cho, Spray pyrolysis deposition of undoped SnO_2 and In_2O_3 films and their structural properties, Prog. Cryst. Growth Charact. Mater. 63 (2017) 1–47.
[48] D.R. Miller, S.A. Akbar, P.A. Morris, Nanoscale metal oxide-based heterojunctions for gas sensing: a Review, Sens. Actuators, B 204 (2014) 250–272.
[49] A. Gurlo, N. Bârsan, A. Oprea, M. Sahm, T. Sahm, U. Weimar, An n- to p-type conductivity transition induced by oxygen adsorption on α-Fe_2O_3, Appl. Phys. Lett. 85 (2004) 2280–2282.

Luís Fernando da Silva is currently Professor at Federal University of São Carlos, Brazil. He received his PhD in Materials and Engineering from São Carlos School of Engineering, University of São Paulo (Brazil) with a Post-doctoral fellowship in the Laboratory for Multifunctional Materials, Department of Materials, at ETH Zürich, Switzerland. His research interests mostly deal with synthesis of MOXs via chemical methods and the characterization of these compounds by X-ray absorption spectroscopy (XAS),

photoluminescence, electron microscopies and the electrical gas-sensing properties of these MOXs.

Ariadne Cristina Catto is currently pos-doctor at Federal University of São Carlos (Brazil), with a fellowship from São Paulo Research Foundation (FAPESP). She received her PhD in Materials and Engineering from São Carlos School of Engineering, University of São Paulo (Brazil). Her research interests mostly deal with synthesis of thin films via chemical and physical methods and the characterization of these compounds by X-ray photoelectron spectroscopy (XPS), atomic force microscopy (AFM), and the gas-sensing properties of these films.

Sandrine Bernardini is a Lecturer at Aix-Marseille University (France). She received(i) her M.S. degree in fundamental physics from Paul Cezanne University, Marseille, France in 1999, (ii) her Engineering degree in materials and microelectronics from the National Institute of Applied Sciences (INSA), Lyon, France, in 2001, and (iii) her Ph.D. degree in microelectronics from Provence University, Marseille, in 2004. From 2005–2007, she moved to the Microelectronic and Nanostructure at the University of Manchester (UK), where she was involved in structural and electrical characterizations to study reliability, interface degradation and impact of high-k dielectrics on carrier transport in MOSFETs. From 2007–2008, she characterized nanometric systems based on zinc oxide nanorods at the Nanoscience Center of Marseille (CINaM). In 2008, she joined the Sensors Group as Lecturer at the Institute Materials and Microelectronic Nanoscience of Provence (IM2NP). Her current interests and activities cover the engineering and physics of gas sensors and selectivity enhancement strategies.

Tomas Fiorido is a Research Engineer at Aix-Marseille University, France. He received his PhD from Paul Cezanne University (France) in2009. The research performed within the framework of this thesis concerned the realization and the characterization of new gas, light and temperature sensors based on polymer material layered over flexible supports. Currently, his research activities are focused on the realization organic or inorganic thin films for sensors, on the engineering of gas microsensors, smoke detector and on the miniature calorimeter for nuclear.

João V. N. de Palma is an undergraduate student in Federal University of São Carlos (UFSCar, Brazil), with a fellowship from Conselho Nacional de Desenvolvimento Científico e Tecnológico (CNPq). The aim of his work is the synthesis and characterization of $Sn_{1-x}Fe_xO_2$ nanostructures.

Waldir Avansi Jr is currently Professor at Federal University of São Carlos, Brazil. He received his PhD in Physics from Institute of Physics of São Carlos (IFSC), University of São Paulo (Brazil). His research interests mostly deals with synthesis of nanostructures via chemical methods and the characterization of these compounds by X-ray absorption spectroscopy (XAS), and advanced techniques of high-resolution transmission electron microscopy.

Khalifa Aguir is a Professor at Aix Marseille University, France. He was awarded his Doctorat d'Etat ès Sciences degree from Paul Sabatier University, Toulouse 1987. He was during the 16 years the head of Microsensors Group at the Institute of Materials Microelectronic Nanosciences of Provence (IM2NP-CNRS) at Aix-Marseille University, Marseille. His principal research interests are directed towards metal – oxide thin films gas microsensors, selectivity, signal treatments and multivariable analysis, modeling, flexible current sensors. He is the author of over 200 publications and international conferences. Referee of several scientific journals, he has conducted numerous expertise and he is a member of scientific committees of international conferences.

Marc Bendahan is a Professor at Aix-Marseille University, France. He is currently the head of the Microsensors Team at the Institute of Materials Microelectronic Nanosciences of Provence and Lecturer at the Institute of Technology. He was awarded his PhD degree from AMU in 1996 with a thesis on shape memory alloys thin films for micro-actuator applications. He is specialized in thin films preparation and characterization for applications in microsystems. His principal research interest is now directed towards the conception, realization and electrical characterization of microsensors: gas microsensors based on inorganic metal-oxides and organic materials, flexible temperature and pressure sensors.